Electronic properties of the Kondo lattice U_2Pt_2Sn

Lan Maria Tran, Bogdan Nowak, and Vinh Hung Tran

Institute of Low Temperature and Structure Research, Polish Academy of Sciences, P.O. Box 1410, PL-50-422 Wrocław, Poland

(Received 26 August 2011; revised manuscript received 27 October 2011; published 12 December 2011)

The magnetization $M(T,H)$, specific heat $C_p(T,H)$, ^{195}Pt and ^{119}Sn NMR Knight shifts $K(T)$, electrical resistivity $\rho(T)$, and magnetoresistance MR(T,H) measurements were performed on a polycrystalline sample of antiferromagnetic compound U_2Pt_2Sn with the Néel temperature $T_N = 15.7$ K. It is found that the $C_p(T)$ and $\rho(T)$ data in the antiferromagnetic state may be interpreted with help of the spin-wave theory with a magnon gap $\Delta/k_B \sim 6$–10 K. Furthermore, analysis of the experimental data allows us to conclude that U_2Pt_2Sn is a dense Kondo system, in which the exchange interaction, Kondo effect, and crystalline electric field compete with each other on the energy scale $T_N < T_K < \Delta_{CEF}$. The Kondo-lattice component of the ^{195}Pt and ^{119}Sn NMR Knight shift has been fitted to the two-fluid model for heavy fermions $K_{KL} \propto (1 - T/T^*)\ln(T^*/T)$ with a characteristic temperature $T^* \sim 80$ K. Electronic properties of heavy-fermion state in U_2Pt_2Sn are discussed in the context of the Wilson ratio ($R_W = 2.8$), Kadowaki-Woods-Tsujii ratio [$A/\gamma^2 \sim 2.15 \times 10^{-5}\ \mu\Omega\,\mathrm{cm/(mJ/mol_U\ K)^2}$ with $N = 2$], and an empirical ratio $R = T^*/T_K \sim 2$.

DOI: 10.1103/PhysRevB.84.224406 PACS number(s): 71.27.+a, 76.60.Cq, 75.30.Mb, 72.15.Qm

I. INTRODUCTION

Uranium-based intermetallics have been intensively studied for many years because of their unusual physical properties at low temperatures, including Kondo effect, heavy-fermion (HF), non-Fermi-liquid (nFl) properties, and unconventional superconductivity. It is generally accepted that these interesting properties arise from the strongly correlated nature of the $5f$ electrons, presumably due to a competition between the intrasite Kondo effect characterized by Kondo energy $k_BT_K \propto \exp(-1/|J|)$ and the intersite magnetic Rudermann-Kittel-Kasuya-Yosida (RKKY)-type exchange interactions with a characteristic energy $k_BT_{RKKY} \propto J^2$. As it was shown by Doniach,[1] within the framework of the Kondo-lattice model, the exchange parameter J, which determines the hybridization strength of f electrons with the conduction electrons, may describe the behavior of f-electron systems, namely, a long-range magnetic ordering with reduced moments is expected to appear at a small J, heavy-fermion behavior at a critical J_{cr}, and nonmagnetic Kondo state for a large J.

From literature,[2–4] and our previous study,[5] we learn that series of the U_2T_2(Sn, In) (T = d-electron transition metal) compounds seem to meet the mentioned Kondo-lattice model. In fact, depending on the f-ligand hybridization strength V_{fd}, one follows the evolution of the magnetic behavior in this series of compounds, and one observes a great variety of electronic correlation phenomena.[5] For instance, with increasing V_{fd}, the Néel temperature increases and presents a maximum value at the V_{fd} of the Pd-based compounds. On the contrary, the Co-, Ru-, and Ir-based compounds with much larger V_{fd} appear to have a nonmagnetic ground state. At the magnetic-nonmagnetic border, there are U_2Pt_2Sn,[3] U_2Pt_2In,[4] and U_2Rh_2In.[6,7] The experimental data reported for U_2Pt_2In (Refs. 8 and 9) pointed out its HF and nFl properties as a consequence of magnetic instability. Owing to the close relationship between U_2Pt_2In and U_2Pt_2Sn, it is thus necessary to study the latter in more detail.

U_2Pt_2Sn was reported to crystallize with the tetragonal Zr_3Al_2-type structure (space group $P4_2/mnm$).[10,11] The measurements of ac magnetic susceptibility of U_2Pt_2Sn indicated an antiferromagnetic (AF) ordering below 15.8 K.[5,12] Subsequent neutron diffraction studies revealed a complex incommensurate noncollinear magnetic structure with the U moments of 1.16 μ_B tilted by 60° from the c axis.[13] U_2Pt_2Sn exhibits a large electronic contribution to the specific heat with the Sommerfeld ratio $\gamma = 334$ mJ/(mole K^2).[3] At higher temperatures, magnetic susceptibility of U_2Pt_2Sn is characterized by the effective moment $\mu_{eff} = 2.86\ \mu_B$ and the paramagnetic Curie temperature $\Theta_p = -141$ K as obtained from the Curie-Weiss law.[14] Electrical resistivity $\rho(T)$ in the paramagnetic state shows a negative temperature coefficient of resistivity, resembling a Kondo-type behavior, while magnetoresistance MR below T_N is negative and displays a steplike decrease around 2 T, probably due to some spin reorientation.[15]

In this study, we focus on U_2Pt_2Sn for the following reason. Not only has the electronic ground state of U_2Pt_2Sn not been investigated enough, but confirming the Kondo effect and exploration of heavy-fermion state in U_2Pt_2Sn may help us in understanding the physical properties of the series of compounds U_2T_2(Sn, In) systematically. Therefore, we have measured magnetization, specific heat, ^{195}Pt and ^{119}Sn NMR Knight shifts, electrical resistivity, and magnetoresistance on a polycrystalline sample of U_2Pt_2Sn. Our measurements show that in the ordered state, the behavior can be described by the spin-wave theory by taking into consideration some ferromagnetic correlations. The energy gap in the magnon spectrum of about 6–10 K was derived from fits of zero-field specific heat and electrical resistivity data. We argue that U_2Pt_2Sn is an antiferromagnetic Kondo lattice in which the Kondo effect with a Kondo temperature of $T_K \sim 30$ K coexists with the crystalline electric field (CEF). Interestingly, we found that the Kondo component of the ^{195}Pt and ^{119}Sn NMR Knight shifts $K(T)$ follow two-fluid scaling law with a characteristic temperature $T^* \sim 80$ K.

II. EXPERIMENTAL DETAILS

Several polycrystalline samples of U_2Pt_2Sn of about 0.5 g each were prepared by arc-melting stoichiometric amounts of the constituents (U: 3N, Pt: 4N, and Sn: 5N) in a Ti-gettered

argon atmosphere. The specimens were remelted several times to ensure good homogeneity. The weight losses during the sample preparation were lower than 0.5% of the total mass. The quality of the samples was checked by microprobe analysis using a Phillips 515 scanning electron microscope equipped with an energy dispersive x-ray (EDX) analysis PV 9800 spectrometer. The microanalysis was performed by collecting several EDX spectra at various locations across the surface of the U_2Pt_2Sn samples. The compositions determined by EDX are U: 38.05, Pt: 41:05, and Sn: 20.90 at. %, thus are close to the ideal composition 2:2:1. No impurity phase within the experimental error is observed in the EDX spectra. X-ray powder diffraction using a Simens powder diffractometer with monochromatized CuK_α radiation ($\lambda = 0.154\ 056$ nm) was performed at room temperature. The x-ray data were analyzed by means of the Rietveld profile procedure using the program WINPLOTR.[16] The observed Bragg peaks can be well indexed to the tetragonal structure with the space group $P4_2/mnm$. The absence of any unindexed peaks indicates an upper limit of impurity phases less than 3 wt %. The refined lattice parameters of U_2Pt_2Sn are $a = 0.7676(5)$ and $c = 0.7411(2)$ nm, and are in good agreement with previously reported values $a = 0.7668$, $c = 0.7389$ nm for a single crystal of U_2Pt_2Sn.[10] In order to get isostructural, nonmagnetic analog to U_2Pt_2Sn, we attempted to prepare Th_2Pt_2Sn and Lu_2Pt_2Sn. However, our experiments have so far been unsuccessful, although most of observed Bragg peaks have similar positions to those of U_2Pt_2Sn, intimating that their crystal structures are closely related.

The dc magnetization measurements $M(T,H)$ were carried out with a Quantum Design MPMS-5 SQUID magnetometer in the temperature range 1.8–400 K and at applied magnetic fields up to 5.5 T. The magnetization data were collected in zero-field-cooled (ZFC) sample mode on three differently field-oriented samples. The bulk sample of about 0.2 g was ground into a fine powder and loaded into a gelatin capsule. The sample prepared by this manner will be named as random oriented. The second was the same powdered sample, but was mixed with GF glue and was oriented by a magnetic field of 5 T at room temperature until the glue dried (we call it field-oriented hereafter). The last sample was measured in magnetic fields perpendicularly to the second one (field-oriented perpendicular). The obtained data on these three samples may present approximately magnetization measured for polycrystalline M_{poly}, along the magnetic easy axis $M_\parallel$, and along the magnetic hard axis $M_\perp$, respectively. The background contribution of the sample holder (gelatin capsule and plastic straw) was separately measured. The accuracy of the measurements was estimated to be within $\pm 1\%$.

The specific heat $C_p(T,H)$ and electrical resistivity $\rho(T,H)$ in applied magnetic field up to 9 T were measured employing a Quantum Design PPMS platform. The C_p data were collected on a sample of 4 mg using a thermal relaxation method in the temperature range 0.4–100 K, whereas ρ data of a bar sample $0.35 \times 1.8 \times 2.1$ mm^3 in the range 1.8–400 K by applying a standard four-probe ac technique. The experimental error of the specific heat and electrical resistivity measurements does not exceed 5%.

To make the NMR measurements, a radio-frequency field penetration of the sample is necessary. Thus, our ^{119}Sn and ^{195}Pt NMR measurements were carried out on a fine powder (~1.5 g) with grain size smaller than rf skin depth. The measurements were performed between 20 and 293 K using a Bruker Avance DSX 300 spectrometer operating at a field of 7.05 T and temperature controller ITC-503 (Oxford Instruments Co Ltd.). The two-pulse sequence (90°_x-τ-90°_y) was applied in order to excite a nuclear spin echo. Preliminary measurements indicated that both ^{119}Sn and ^{195}Pt spectra are asymmetric and extend over more than 0.6 MHz at room temperature. Such spectra are difficult to irradiate uniformly. Then, in order to record correctly the total spectrum, so-called frequency-swept NMR spectra were obtained point by point by changing the irradiating frequency. The NMR probe was returned at each point. Quadrature detection and phase cycling procedures were used throughout. According to IUPAC unified scale,[17,18] ^{119}Sn and ^{195}Pt chemical shift (Knight shift) K should be determined with reference to $\Xi^{119}\text{Sn} = 0.372\ 906\ 32$ and $\Xi^{195}\text{Pt} = 0.214\ 967\ 84$, respectively. Here, Ξ is defined as the ratio of the isotope-specific frequency to that of ^1H in tetramethylsilane (TMS) in the same magnetic field. However, according to the discussion presented in Ref. 19 and references therein, in this paper we express the ^{195}Pt Knight shifts (in %) as $^{195}K = {}^{195}K[\Xi(^{195}Pt) + 0.63]$.

III. RESULTS

A. Magnetic properties

In Fig. 1(a), we compare temperature dependence of the inverse magnetic susceptibility $\chi^{-1}(T) \equiv (M/H)^{-1}(T)$ for field-oriented and field-oriented perpendicular samples of U_2Pt_2Sn at a field of 5 T. In order to determine magnetic parameters, we have fitted the experimental data to a Curie-Weiss law $\chi(T) = \frac{N_A}{3k_B}\frac{\mu_{\text{eff}}^2}{(T-\Theta_p)}$. Above 200 K, the Curie-Weiss fit describes $\chi(T)$ data reasonably, e.g., the effective moment $\mu_{\text{eff}} = 3.21 \pm 0.05\ \mu_B$/U and a paramagnetic Curie temperature $\Theta_p = -160 \pm 5$ K were obtained from the fit of the $\chi_\parallel(T)$ data. However, a careful look at fitting reveals that the fitting parameters depend strongly on the temperature range in which the fit was done; μ_{eff} may increase up to 3.28 μ_B if taking data in the temperature range 300–400 K for fits. It turns out that the experimental data are better described by a modified Curie-Weiss (MCW) law $\chi(T) = \chi_0 + \frac{N_A}{3k_B}\frac{\mu_{\text{eff}}^2}{(T-\Theta_p)}$. Within the MCW fit of the data in a wider temperature range, i.e., between 80 and 400 K, we obtain $\chi_0 = 0.61 \pm 0.03 \times 10^{-3}$ cm^3/mol$_U$, $\mu_{\text{eff}} = 2.32 \pm 0.04\ \mu_B$/U, and $\Theta_p = -66 \pm 5$ K from the $\chi_\perp(T)$ data, and $\chi_0 = 0.66 \pm 0.02 \times 10^{-3}$ cm^3/mol$_U$, $\mu_{\text{eff}} = 2.46 \pm 0.05\ \mu_B$/U, and $\Theta_p = -58 \pm 4$ K from the $\chi_\parallel(T)$ data. The presence of the temperature-independent susceptibility χ_0 is usually interpreted as contributions of conduction electrons (Pauli susceptibility) and from transitions between ground-state and excited orbitals in ions with partially filled electronic shells (Van Vleck paramagnetism). The effective moment deduced from our measurements is comparable with the literature data [2.03 μ_B (Ref. 14) and 2.86 μ_B (Ref. 3)] or with intermediate coupling values expected for free U^{3+} (2.55 μ_B) or U^{4+} (3.34 μ_B) ions. The negative sign of the Θ_p values indicates antiferromagnetic exchange interactions between the magnetic uranium ions. However, a relatively

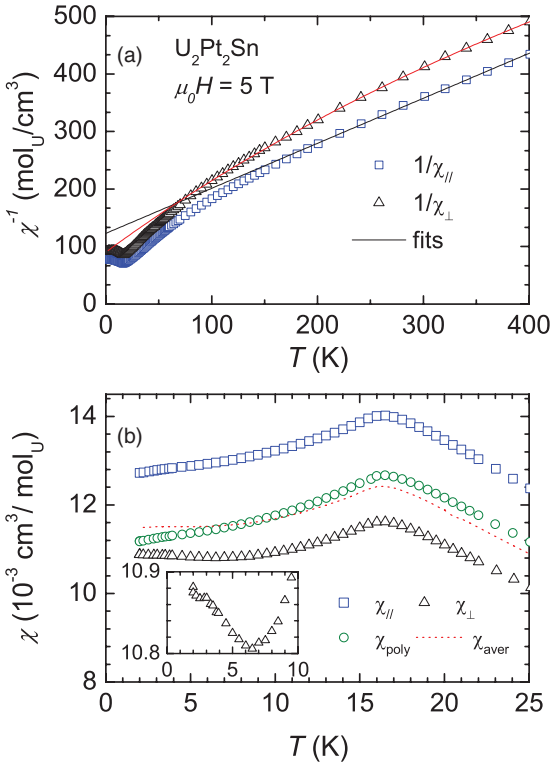

FIG. 1. (Color online) (a) A comparison of temperature dependence of the inverse magnetic susceptibility of field-oriented and field-oriented perpendicular samples of U_2Pt_2Sn at 5 T. The solid lines are fits to the Curie-Weiss law or modified Curie-Weiss law. (b) Temperature dependence of the low-temperature susceptibility. The dashed line is the calculated average susceptibility. The inset shows the part of $\chi_\perp$ below 10 K on enlarged scales.

large absolute value additionally implies the presence of the Kondo effect. The value of paramagnetic Curie temperature in such a case is related to the Kondo temperature T_K via the relation $T_K \sim |\Theta_p|/m$, where $m = 1$–4, depends on the choice of the different theoretical models.[20] Albeit, from the theoretical point of view, the relationship between T_K and Θ_p should be valid only for paramagnetic Kondo compounds, the experimental data, however, have demonstrated that it may be applied in magnetically ordered systems too.[21,22] Θ_p of U_2Pt_2Sn deduced from our susceptibility data amounts to about -60 K, thus may provide a value of $T_K \sim 15$–30 K.

The low-temperature magnetic susceptibility at 5 T as a function of temperature is shown in Fig. 1(b). In accord with the literature reports,[3,14] only one pronounced maximum manifesting an antiferromagnetic phase transition is found in the $\chi(T)$ curves. Using Fisher's method for itinerant antiferromagnets,[23] we determined the Néel temperature for U_2Pt_2Sn as the maximum of the derivative of the product $[\chi(T)T]$ to be $T_N = 15.6$ K at 5 T. Comparison of the calculated average susceptibility $\chi_{av} = (2 \cdot \chi_\perp + \chi_\parallel)/3$ with that of random-oriented sample χ_{poly} reveals fairly good agreement, suggesting a good crystalline orientation of measured samples. As can be seen from the figure, U_2Pt_2Sn does show a weak magnetocrystalline anisotropy, reflected by small values of ratio $\chi_\parallel/\chi_\perp$. At T_N, it amounts to 1.2 and goes down to 1.1 at room temperature. Nevertheless, the existing anisotropy exhibits different temperature dependencies of $\chi(T)$ curves. Unlike $\chi_\parallel(T)$ dependence, $\chi_\perp(T)$, displayed on an enlarged scale in the inset, shows an upturn increase below 7 K, implying the existence of ferromagnetic correlations.

B. Specific heat

The dependence of the specific heat of U_2Pt_2Sn divided by temperature C_p/T versus T is shown by closed symbols in Fig. 2. The data are dominated by a pronounced λ-type anomaly at 15.7 K, ascertaining the Néel temperature of U_2Pt_2Sn. To quantitatively analyze the data, one assumes the specific heat to be additive, being the sum of at least three distinct components: the phonon specific heat C_{ph}, the $5f$-electron contribution C_{5f}, and the electronic specific heat C_{el}. The latter was taken as linearly temperature dependent $C_{el} = \gamma T$. Since no samples of isostructural, non-f-electron compound were available, the phonon contribution to the specific heat could not exactly be estimated. However, an approximation can be provided if one assumes $C_{ph}(T)$ of U_2Pt_2Sn to be the renormalized phonon specific heat of Th_2Ru_2Sn. Taking into account the Debye temperature of Th_2Ru_2Sn [$\Theta_D(Th_2Ru_2Sn) \sim 210$ K (Ref. 24] and difference between the molar masses of Th_2Ru_2Sn and U_2Pt_2Sn, we have estimated the Debye temperature of U_2Pt_2Sn $\Theta_D(U_2Pt_2Sn)$, using the formula[25]

$$\Theta_D(U_2Pt_2Sn) = \Theta_D(Th_2Ru_2Sn) \times \left[\frac{2m(Th)^{3/2} + 2m(Ru)^{3/2} + m(Sn)^{3/2}}{2m(U)^{3/2} + 2m(Pt)^{3/2} + m(Sn)^{3/2}}\right]^{1/3}, \quad (1)$$

where m(X) are the molar masses of X atoms, respectively. The estimated Debye temperature of U_2Pt_2Sn amounts to $\Theta_D(U_2Pt_2Sn) \sim 189.8$ K. A similar order of magnitude of Θ_D was considered for other 221 compounds, e.g., U_2Pt_2In ($\Theta_D = 175$ K),[4] U_2Rh_2In ($\Theta_D \sim 180$ K),[7] U_2Pd_2In ($\Theta_D = 185$ K), and U_2Pd_2Sn ($\Theta_D = 212$ K).[26] In Fig. 2, we show the estimated phonon specific heat of U_2Pt_2Sn $C_{ph}(T)$ (J/mol_U K),

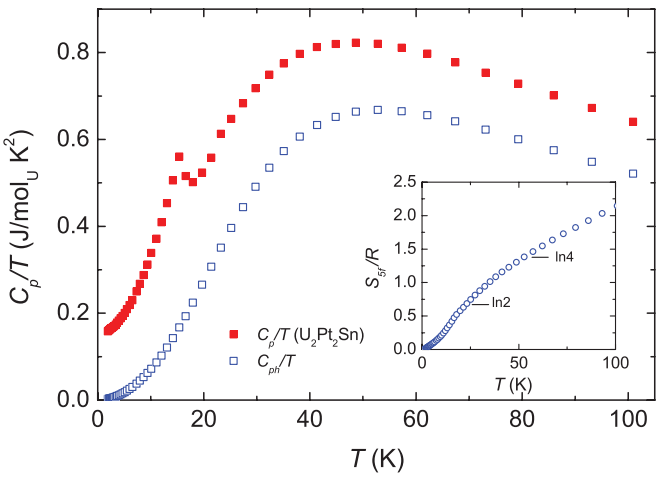

FIG. 2. (Color online) The total and phonon specific heats divided by temperature of U_2Pt_2Sn as a function of temperature. The inset shows the $5f$-electron entropy S_{5f}/R vs T.

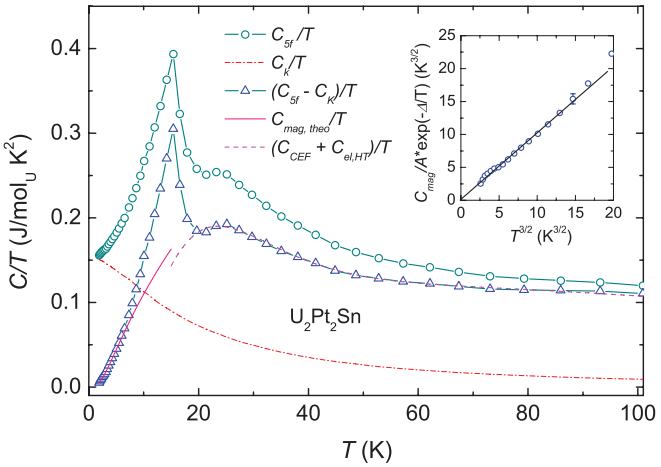

FIG. 3. (Color online) Comparison of $5f$-electron specific heat of U_2Pt_2Sn with calculated CEF, Kondo, and magnon contributions. The inset illustrates the presence of $T^{3/2}$ term in the magnetic specific heat.

which is modeled by the Debye function[27]

$$C_{ph}(T) = 9Rn_D(T/\Theta_D)^3 \int_0^{\Theta_D/T} \frac{x^4 \exp(x)}{[\exp(x)-1]^2} dx, \quad (2)$$

where R is the molar gas constant and $n_D = 2.5$ is the number of Debye vibrators.

We may evaluate the $5f$ contribution $C_{5f}(T)$ to the total specific heat by subtracting the phonon specific heat $C_{ph}(T)$ of U_2Pt_2Sn, and then calculate the $5f$-electron entropy $S_{5f}(T) = \int_0^T \frac{C_{5f}(T)}{T} dT$. The value of S_{5f} at T_N is only $\simeq$64% of the expected Rln2 value for a ground-state doublet (see inset of Fig. 2). This observation may be an indication of the influence of the Kondo effect, due to which not all the electronic degrees of freedom are condensed into magnetic ordered ground state.

Further support to the presence of the Kondo effect can be obtained from an analysis of $C_{5f}(T)/T$ shown as open circles in Fig. 3. Apparently, $C_{5f}(T)/T$ exhibits an enhancement in the Sommerfeld ratio C_p/T, both at low temperatures and at $T > T_N$. A large $\gamma = C_p/T$ value extrapolated to $T = 0$ K, of the order of 150 mJ/mol$_U$ K^2, suggests that there will be a corresponding enhanced effective mass m^*. According to the formula

$$m^* = \frac{3\hbar^2 \gamma_V}{k_B^2 k_F}, \quad (3)$$

where Fermi wave vector $k_F = (3\pi^2 Z/\Omega)^{1/3} = 1.176 \times 10^{10}$/m, $Z = 24$ is the number of conduction electrons, assuming that there are three heavy $5f$ electrons per U atom, Ω is the volume of the unit cell divided by the formula unit per cell, and the volumetric coefficient of the electronic specific heat $\gamma_V = 4.563$ J/m^3 K^2, the effective mass reaches $\sim 75\, m_e$, where m_e is the free electron mass. This result indicates that the $5f$ electrons contribute dominantly to the density of states at the Fermi level, and this is essentially a result of the formation of coherent Kondo resonance at low temperatures. Therefore, it is of interest to estimate the characteristic Kondo temperature T_K of the system. We used an approach of Bredl *et al.*[28] within a mean-field theory. As shown by Blanco *et al.*,[29] T_K and T_N are related via the formula

$$\Delta C = \frac{6k_B}{\Psi'''\left(\frac{1}{2}+\zeta\right)} \left[\Psi'\left(\frac{1}{2}+\zeta\right) + \zeta\Psi''\left(\frac{1}{2}+\zeta\right)\right]^2, \quad (4)$$

where $\zeta = \frac{T_K}{2\pi T_N}$ and Ψ', Ψ'', and Ψ''' are the first three derivatives of the digamma function. Applying Eq. (4) for the specific-heat jump ΔC at T_N $\Delta C(15.7\ \text{K}) = 3.1$ J/mol$_U$ K, we obtain $T_K = 29$ K. Another way of obtaining T_K is to use the expression given by Yashima *et al.*[30]:

$$S\left(\frac{T_K}{T_N}\right) = R\left\{\ln\left[1+\exp\left(-\frac{T_K}{T_N}\right)\right] + \frac{T_K}{T_N}\frac{\exp\left(-\frac{T_K}{T_N}\right)}{1+\exp\left(-\frac{T_K}{T_N}\right)}\right\}. \quad (5)$$

For U_2Pt_2Sn, the $5f$-electron entropy at T_N is 3.51 J/mol$_U$ K, which yields $T_K = 28$ K. The next support for the presence of the Kondo effect in U_2Pt_2Sn arises from comparison of the $5f$-electron specific heat with Kondo contribution C_K inferred from the solution of the Coqblin-Schrieffer (CS) model for $J = 1/2$ by Rajan.[31] In the CS model, the characteristic temperature T_K, which accounts for the energy scale of the Kondo interaction, is given by a relation $T_K = (N-1)\pi R/6\gamma$, $N = 2J+1$. Setting the quantum number $J = 1/2$ and $\gamma = 150$ mJ/mol$_U$ K^2, we derive $T_K = 29$ K. These T_K values estimated from three different approximations are in good agreement with one another. We may add that the eventual error resulting from the not well-defined phonon specific heat has a minor effect on the jump ΔC value at T_N and the coefficient of the electronic specific heat γ, supporting that the Kondo effect with the Kondo temperature $T_K \sim 29$ K has to be taken into account in order to describe the ground-state properties of U_2Pt_2Sn. We show the Kondo contribution $C_K(T)$ to $C_{5f}(T)$ as dashed-dotted line in Fig. 3. We calculated the magnetic specific heat according the formula $C_{\text{mag}}(T) = C_{5f} - C_K(T)$, as shown as open triangle symbols in Fig. 3. The antiferromagnetic phase transition is clearly shown in Fig. 3. In the magnetically ordered state, the magnetic specific heat may be regarded as the consequence from spin-wave contribution. There are several exponential dependencies that have been proposed[27,32,33]:

$$C_{\text{mag}}(T) = f(T)\exp(-\Delta/k_BT), \quad (6)$$

where $f(T) = T^n$ is a power-law function with n dependent on the nature of the spin waves and Δ is the spin-wave gap in the magnon spectrum. Our attempts to fit the C_{mag} data to Eq. (6), using $n = 3$ or $-1/2$ predicted for an antiferromagnet, fail completely. Instead, an analysis of the data below 7 K does show a $C_{5f}(T) = AT^{3/2}\exp(-\Delta/k_BT)$ dependence with $a = 0.061$ ($\pm$ 0.004) J/mol$_U$ K$^{5/2}$ and $\Delta/k_B = 6 \pm 0.6$ K (solid line shown in Fig. 3). The presence of $T^{3/2}$ (see inset of Fig. 3) is probably due to considerable ferromagnetic interactions. Such a behavior is not unusual for antiferromagnets. Previously, $C_{\text{mag}} \propto T^{3/2}$ was found in several antiferromagnetic compounds with ferromagnetic correlations, such as $CePd_{0.9}Ag_{0.1}$ and $CePd_3Ga_2$.[34]

As can be seen from Fig. 3, the Kondo effect with $T_K = 29$ K may account for the enhancement in the $C_{5f}(T)/T$ ratio at low temperatures but is not able to explain a large value of $C_{5f}(T)/T$ above T_N. We suspect that the $5f$-electron specific heat in the paramagnetic state with a broad maximum $T_{\max} \sim 25$ K would have a sizable contribution from crystal electric field effect, and in principle, also from high-temperature electronic specific heat C_{el}. The presence of CEF effect in several uranium intermetallics was previously documented by specific-heat measurements, for instance, UBe_{13},[35] U_2Zn_{17},[36] and UPd_3.[37] In the U_2Pt_2Sn unit cell, two uranium atoms occupy two atomic positions *4g* and *4f*, each having the orthorhombic *mm2* local symmetry (C_{2v} group). In such a symmetry, the multiplet $J = 9/2$ for U^{3+} may split into five Kramers doublets, while the $J = 4$ state for U^{4+} may have nine singlets. If a tetragonal distortion occurs at low temperatures, two non-Kramers doublets and five singlets are expected. In any case, a doublet as a ground state is required for magnetic state of U_2Pt_2Sn. Assuming a three-level scheme with a doublet as the ground state, and the first and second excited CEF levels corresponding to either or single, doublet, or triplet, we have fitted the data to the equation[27]

$$C_{\mathrm{CEF}}(T) = R\frac{\sum_{i=1}^{2} g_0 g_i \left(\frac{\Delta_i}{k_B T}\right)^2 \exp\left(-\Delta_i/k_B T\right) + g_1 g_2 \left(\frac{(\Delta_2-\Delta_1)}{k_B T}\right)^2 \exp\left[(\Delta_1-\Delta_2)/k_B T\right]}{\left[\sum_{i=0}^{2} g_i \exp(-\Delta_i/k_B T)\right]^2}, \tag{7}$$

where g_i, $i = 0,1$, and 2, are the degeneracies of the CEF levels with the corresponding splitting energies $\frac{\Delta_i}{k_B}$. In order to get reasonable fitting parameters, we fixed $g_0 = 2$ and limited Δ_1/k_B in the range $T_{\max}/0.3$–$T_{\max}/0.4$, whereas g_1, g_2, and Δ_2 were allowed to vary independently. In Fig. 3, we show the result of the fitting with $g_1 = 2$, $g_2 = 3$, $\Delta_1/k_B = 76 \pm 1$ K, and $\Delta_2/k_B = 380 \pm 10$ K. It appears from the fits that the $5f$-electron specific heat may also contain the $C_{el} = \gamma_{HT} T$ contribution. However, the latter linear term has an essentially large coefficient of 55 $\mathrm{mJ/mol_U\ K^2}$, i.e., about several times higher than expected. One of the possible reasons is that the lattice contribution to the specific heat from the Debye phonon specific heat was underestimated. Although the agreement between the theoretical and experimental data in the fits seemed quite satisfied, we must admit that our evaluation is merely a phenomenological model that accounts for the experimental specific-heat results. A more suitable microscopic description of the magnetic state of U_2Pt_2Sn should be acquired from inelastic neutron scattering data, which are underway.

In Fig. 4, the Sommerfeld ratio at 0.4 K in various magnetic fields up to 9 T is shown. $C_p(T)/T$ at 0.4 K amounts to 160 $\mathrm{mJ/mol_U\ K^2}$ at zero field. Upon applied fields, $C_p(H,T)/T$ at 0.4 K shows a minimum at 1.8 T and followed by weak enhancement with further increasing fields. Because magnetic fields usually lower the Kondo specific heat C_K, the field dependence of $C_p(H,T)/T$ at 0.4 K up to 1.8 T may be explained by the presence of Kondo effect. For the data at high magnetic fields, an increase of magnon contribution and/or spin reorientation are possible mechanisms generating the increasing tendency of the $C_p(H,T)/T$ at 0.4 K. In antiferromagnets, magnetic fields depress T_N to lower temperatures, thus may increase magnetic specific heat. Further investigation appears necessary to delineate the field-dependence behavior.

C. ^{195}Pt and ^{119}Sn NMR

In the space group $P4_2/mnm$, Pt and Sn atoms occupy the positions with monoclinic and tetragonal site symmetries, respectively. Thus, both the ^{195}Pt and ^{119}Sn frequency-swept NMR spectra are slightly asymmetric, promising an anisotropy in the Knight shifts. However, the spectra are very broad due to macroscopic magnetism of the sample at a field 7.05 T. In Fig. 5, the NMR spectrum of ^{195}Pt nuclei at room temperature is shown. Owing to large resonance shifts being to about one

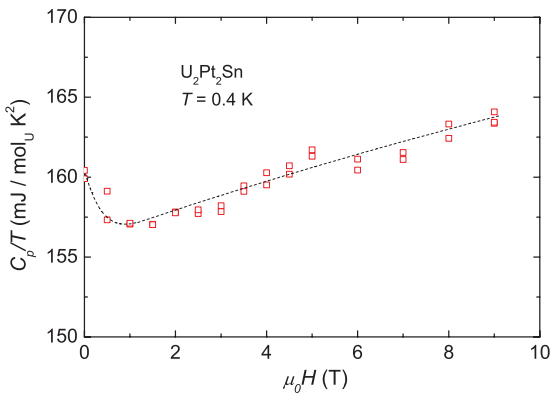

FIG. 4. (Color online) Field dependence of the Sommerfeld ratio at 0.4 K. The dashed line is a guide for the eye.

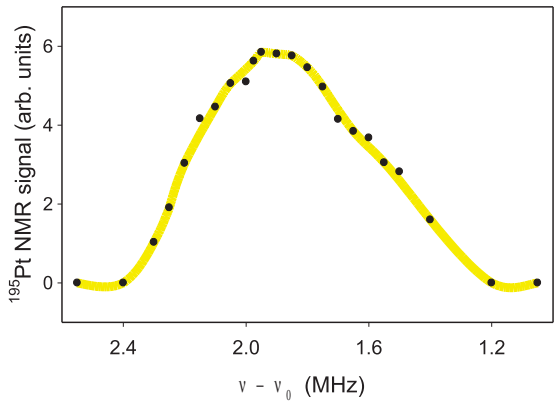

FIG. 5. (Color online) NMR ^{195}Pt spectrum of U_2Pt_2Sn at room temperature.

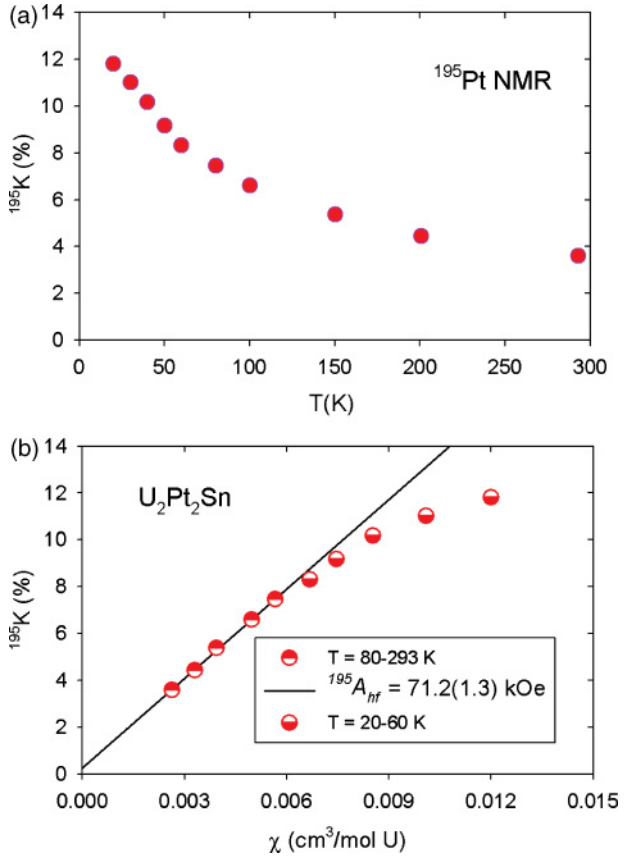

FIG. 6. (Color online) (a) Temperature dependence of shift of ^{195}Pt nuclei in U_2Pt_2Sn. (b) The Knight shift of ^{195}Pt nucleus versus magnetic susceptibility. The solid line is a fit to the high-temperature data above 80 K.

order of magnitude larger than the line width, the maximum of the spectrum is well defined. To determine the Knight shift, the maximum of the spectrum corresponding to isotropic value $^{195}K_{\rm iso}$ was measured. It is found that the shifts have very large positive values. ^{195}K amounts to 11.8% at 20 K and diminishes with increasing temperature (see upper panel of Fig. 6).

In magnetic f-electron intermetallics, where the susceptibility changes with temperature, one can separate the Knight shift into a temperature-dependent term K_f due to the f electrons and a temperature-independent term K_0, being the sum of an orbital component $K_{\rm orb}$ and a contribution from the conduction-electron spins $K_{\rm CE}$. We therefore write

$$K(T) = K_0 + K_f(T). \tag{8}$$

In Fig. 6(b), the ^{195}Pt Knight shift ^{195}K(T) is plotted against the bulk magnetic susceptibility $\chi(T)$, with temperature as the implicit parameter. This plot is justifiable by the usual relationship existing between Knight shift and molar susceptibility in the paramagnetic state[38]

$$K_f(T) = (\mu_B N_A)^{-1} A_{hf}\chi(T). \tag{9}$$

Here, A_{hf} is the static transferred hyperfine coupling constant, which represents a local field experienced by the ligand nuclei, induced on each U ion by the applied field in the paramagnetic state. If a single mechanism dominates the temperature dependence of both the susceptibility and Knight shift only, we should observe a straight line of the $K(T)$ versus $\chi(T)$ curve since A_{hf} is independent of temperature. It is the case for U_2Pt_2Sn at temperature above $T^* = 80$ K. From the linearity of the $K(T)$ versus $\chi(T)$ curve, we obtain for ^{195}Pt nuclei in U_2Pt_2Sn the hyperfine coupling constant $^{195}A_{hf} = +71.2$ kOe/μ_B. The isotropic component $^{195}A_{hf}$ represents the transferred hyperfine interaction between the U 5f orbitals and the Pt 6s and 5d orbitals. The observed magnitude and sign of the transferred hyperfine coupling results from a competition between them. The 6s(Pt)-5f(U) mixing produces a positive contribution to the hyperfine field at the ^{195}Pt nuclei. On the other hand, the net spin moment of the 5d electrons at the Pt site is parallel to the moment of the 5f electrons at the U site. These spin-polarized d electrons then polarize the inner-core s electrons, producing negative hyperfine field through the Fermi contact interaction between the ^{195}Pt nucleus and the core-s electrons. Uranium- and rare-earth-based intermetallics are known to exhibit both positive and negative values of $^{195}A_{hf}$. For instance, negative $^{195}A_{hf}$ values were found in UPt_3 (Refs. 39 and 40) and UPtSn,[41] whereas positive ones are in $U_3Pt_3Sn_4$,[42] $CePt_4In$,[43] and in UPt_2Si_2.[44] In U_2Pt_2Sn, the large and positive value of transferred hyperfine coupling constant implies the dominant role of the 6s(Pt)-5f(U) mixing process.

We must admit that the components $K_\parallel$, $K_\perp$, and thus $K_{\rm iso} = (1/3)(K_\parallel + 2K_\perp)$ of the axially symmetric ^{119}Sn Knight shift in U_2Pt_2Sn can not be reliably determined due to severe magnetic broadening of the NMR line at 7.05 T and weak signal intensity associated with natural abundance of ^{119}Sn nuclei of only 8.59%. To overcome the problem, the Knight shift of ^{119}Sn was then measured at the peak of the very large spectrum, i.e., at the frequency in the spectrum corresponding roughly to the singularity in the powder pattern due to grains oriented perpendicular to the field ($\approx^{119}K_\perp$). Since the axial Knight shift $K_{ax} = (1/3)(K_\parallel - K_\perp)$ is probably small, as deduced from the magnetization measurements of field-oriented and field-oriented-perpendicular samples of U_2Pt_2Sn, the measured ^{119}K should not differ significantly from $K_{\rm iso}$. We found that the shift $^{119}K(T)$ has very large positive value of + 10.5% at 20 K (Fig. 7). In a similar manner as ^{195}K does, the $^{119}K(T)$ versus $\chi(T)$ curve shown in Fig. 7 is linear for $T > 80$ K. Using Eq. (9), we obtain $^{119}A_{hf} = +61.3$ kOe/μ_B, which is caused by the polarization of Sn 5s conduction electrons by U 5f electrons through the s-f hybridization. The obtained value is slightly larger than those found in UTSn (T = Pt, Ni),[41,45] crystallizing in the cubic MgAsAg-type structure or larger than those of $U_3T_3Sn_4$,[42,45,46] adopting the cubic $Y_3Au_3Sb_4$ type of structure.

We emphasize that the K versus χ curves of ^{195}Pt and ^{119}Sn behave very similarly to one another, i.e., linear dependence for $T > 80$ K and a deviation from the linearity below 80 K. This observation points to a common physical mechanism for the Knight shifts. In Fig. 8, we plot $^{119}K(T)$ versus $^{195}K(T)$. As can be seen, the full correlation exists between $^{119}K(T)$ and $^{195}K(T)$ over the whole temperature range of measurements, suggesting that the deviation from linearity of $K(T)$ versus $\chi(T)$ curves observed below T^* is an intrinsic property of U_2Pt_2Sn, and indicates a change in the A_{hf} value.

In many 4f and 5f heavy-fermion compounds, deviation was already observed of the $K(T)$ versus $\chi(T)$ plot from

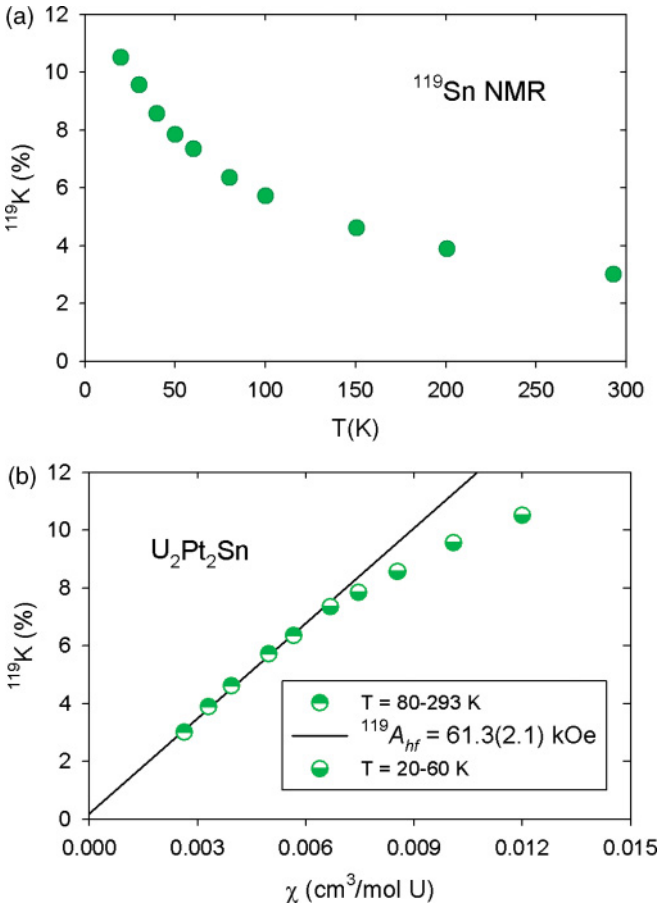

FIG. 7. (Color online) (a) Temperature dependence of the Knight shift of ^{119}Sn nucleus in U_2Pt_2Sn. (b) The Knight shift of ^{119}Sn nucleus versus magnetic susceptibility. The solid line is a fit to the high-temperature data above 80 K.

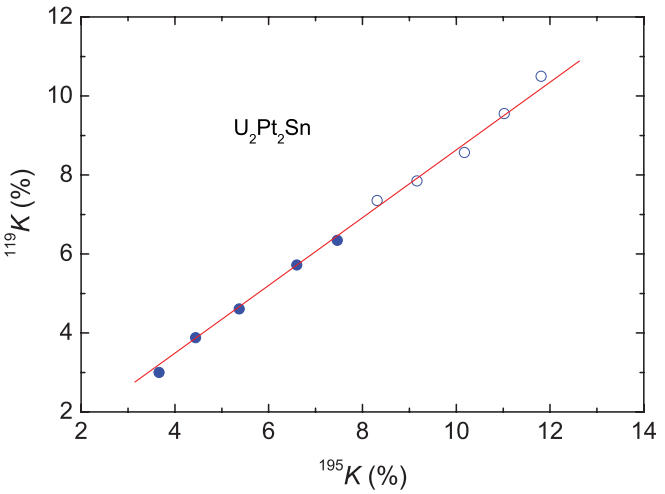

FIG. 8. (Color online) Relationship between the experimental Knight shifts of ^{119}Sn and ^{195}Pt nucleus in U_2Pt_2Sn. The closed and open symbols represent data above and below T^*.

its linear relation at low temperatures.[47–57] Two different mechanisms have been proposed to explain this deviation in heavy-fermion systems: one is based on the fact that the effective hyperfine coupling f-c has been modified by crystalline electric field, and the other is related to the onset of Kondo compensation below a characteristic temperature T^*. In $CeAl_3$,[47] $CeCu_2Si_2$,[50] UNi_2Al_3, and UPd_2Al_3,[51] the effect has been interpreted as due to the depopulation of an excited CEF level of the magnetic ions. The orbital overlap of f and ligand atoms depends on the CEF-level population. Thus, it provides additional temperature-dependent hyperfine coupling to NMR nuclei. The CEF model considers the influence of the population of the levels of the CEF on the hyperfine coupling constant, thus is able to explain the change in the sign of A_{hf}. In $CeCu_2Si_2$,[50] it was suggested that A_{hf} can become negative when only the lowest CEF doublet is occupied. In U_2Pt_2Sn, the lowest CEF doublet becomes fully occupied at temperature about 30 K, where the magnetic entropy reaches a value of ln 2. At this temperature, no change in sign of A_{hf} was observed.

Within the second approach, a two-fluid model has been developed and successfully tested for heavy-fermion and mixed valent systems.[52–57] The two-fluid model postulates the coexistence of the local moment (LM) f-electron lattice with the itinerant heavy-electron Kondo liquid (KL) that emerges through its collective hybridization with the conduction-electron sea below a characteristic temperature T^*. The two-fluid description separates the collective excitations of the Kondo lattice from the individual behavior of localized f spins. According to Curro *et al.*,[54,55] below T^* the local moments and conduction electrons begins to hybridize, but retain both local and itinerant character and thus both Kondo liquid $\chi_{KL}(T)$ and Curie-Weiss $\chi_{LM}(T)$ susceptibilities contribute to the Knight shift with different weights. The magnetic shift arising from the Kondo liquid is given by

$$K_{KL}(T) = K(T) - K_0 - B\chi_{CW}(T) = (A - B)\chi_{KL}(T) \tag{10}$$

and has been shown experimentally to scale as T/T^* below T^*. In Eq. (10), A is an onsite hyperfine tensor interaction to the itinerant electron spin, and B, in the commonly used convention, is a transferred hyperfine tensor A_{hf} to the localized f spins. We find that for our U_2Pt_2Sn sample, the hybridized component χ_{KL} and thus K_{KL} also exhibit

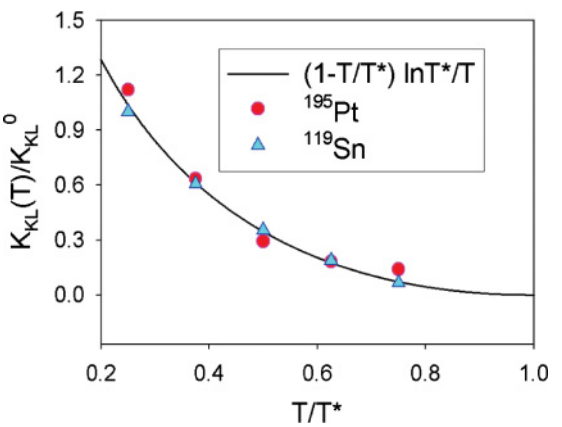

FIG. 9. (Color online) $K_{KL}(T)/K^0_{KL}$ versus $\ln(T/T^*)$ showing the scaling behavior of the Kondo-liquid component of susceptibility. The solid line is given by Eq. (11).

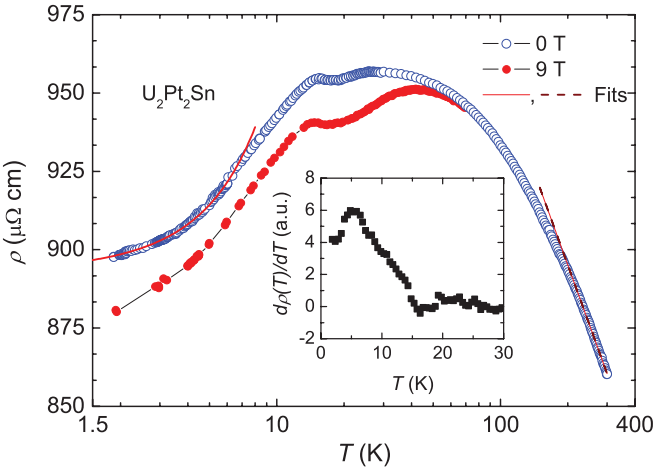

FIG. 10. (Color online) The temperature dependence of the electrical resistivity of U_2Pt_2Sn at 0 and 9 T. The solid line indicates a fit to Eq. (13). The dashed line displays a lnT dependence. The inset shows the temperature derivative of the resistivity of U_2Pt_2Sn.

the scaling form derived in Refs. 54 and 55:

$$K_{\mathrm{KL}}(T)/K^0_{\mathrm{KL}} = (1 - T/T^*)\ln(T^*/T). \tag{11}$$

The result of a fit to Eq. (11) is shown in Fig. 9. The agreement between the experimental data and the two-fluid model is surprisingly good, suggesting that the low-temperature dependence of $^{119}K(T)$ and $^{195}K(T)$ in U_2Pt_2Sn are possible, to be explained by the two-fluid model with $T^* \sim 80$ K.

D. Electrical resistivity and magnetoresistance

The temperature dependence of the electrical resistivity $\rho(T)$ of U_2Pt_2Sn is displayed in Fig. 10. A comparison to the reported data[15] reveals that the overall behavior of the $\rho(T)$ curve is similar one to another, except for a little difference in the ratio $\rho(25\ \mathrm{K})/\rho(2\ \mathrm{K})$ values. Both the and literature and our data point out that U_2Pt_2Sn has a high electrical resistivity, which may be attributed to a low carrier concentration density. From the resistivity data, it is evident that the increase of $\rho(T)$ with decreasing temperature from room temperature is governed by an incoherent Kondo scattering mechanism. In fact, in the temperature range 200–300 K, $\rho(T)$ exhibits a $\rho_K \propto -\ln T$ dependence, as shown by the dashed line in Fig. 10. Obviously, in order to determine precise Kondo contribution ρ_K, one needs to subtract the phonon resistivity from the total resistivity. Unfortunately, this task is not easily performed at the present stage.

With further decreasing temperature, the resistivity passes a broad maximum around 25 K (Fig. 10), indicating coherence effects overcoming single-ion incoherent Kondo scattering. In the Kondo-lattice system, the presence of a maximum in the electrical resistivity is also an indication of the interplay between Kondo and CEF effects. After showing precursor behavior around T_N, which resembles the spin-density wave in Cr,[58] the resistivity drops rapidly due to the antiferromagnetic ordering. Below $T_N/2 \sim 8$ K, the resistivity does not follow a simple Fermi-liquid behavior $\rho(T) \propto AT^2$, suggesting that an additional electron-magnon scattering should be taken into account. The magnon resistivity is described by

$$\rho_{\mathrm{mag}} = f(T,\Delta)\exp(-\Delta/k_BT), \tag{12}$$

where $f(T,\Delta)$ is a prefactor function determining electron-magnon scattering and Δ is the magnon gap energy. We have attempted to fit the data with functions $f(T,\Delta)$ given by Continentino *et al.*[59] and by Jobiliong *et al.*,[60] but goodness of fits was not satisfied. For U_2Pt_2Sn, we applied the function $f(T,\Delta) = BT(1 + \frac{2k_BT}{\Delta})$,[61] previously used for URu_2Si_2 (Ref. 62) and $CePt_3Si$.[63] At low temperatures, neglecting the phonon resistivity, the electrical resistivity in the presence of electron-magnon scattering is approximately expressed as

$$\rho(T) = \rho_0 + AT^2 + BT\left(1 + \frac{2k_BT}{\Delta}\right)\exp(-\Delta/k_BT). \tag{13}$$

A solid line in Fig. 10 shows a fitting curve with fitting parameters $\rho_0 = 901 \pm 3\ \mu\Omega$ cm, $a = 0.48 \pm 0.05\ \mu\Omega$ cm/K^2, $B = 1.8 \pm 0.2\ \mu\Omega$ cm/K, and $\Delta/k_B = 10.4 \pm 5$ K. The obtained gap value is somewhat larger than that from the specific-heat measurement.

A comparison of the resistivity data at 0 and 9 T shows that T_N is shifted to lower temperatures by applied fields. It is a consequence of the disrupting effect of the magnetic field on the antiferromagnetic alignment of the magnetic uranium moments. The applied magnetic field causes decrease of the resistivity and a shift of the resistivity maximum to higher temperatures. This behavior may be readily understood as the behavior expected for a Kondo lattice since the quenching of the Kondo interaction by external magnetic fields lowers the scattering intensity and thus reduces $\rho(T)$.

The magnetoresistance, defined as

$$\mathrm{MR}(T,H) = \frac{\rho(T,H) - \rho(T,0)}{\rho(T,0)}100\%,$$

as a function of applied magnetic fields at selected temperatures in the paramagnetic state is shown in Fig. 11. The isothermal MR curves in the paramagnetic regime exhibit characteristic single-ion Kondo type predicted by Schlottmann.[64] The resistivity at $T = 0$ in a field as function of occupation numbers n_f of the f level is given by Friedel's sum rule:

$$\frac{\rho(T,0)}{\rho(T,H)} = \frac{1}{2J+1}\sin^2\left[\frac{\pi n_f}{2J+1}\right]\sum_{l=0}^{2J}\sin^{-2}(\pi n_l). \tag{14}$$

For $\sum_{l=0}^{2J} n_l = n_f = 1$ and $J = 1/2$, Andrei[65] and Schlottmann[64] obtained the results of the Bethe ansatz calculations for the magnetoresistance [Eq. (14)], from which a characteristic field H^* is derived. The results of fits of our data for T 40 K are given as solid lines in Fig. 11. The temperature dependence of the characteristic field H^*, which involves Kondo temperature, is shown in Fig. 11(b). According to Batlogg,[66] H^* is given as

$$\mu_0 H^* = \frac{k_BT}{g\mu_K}(T_K + T), \tag{15}$$

where g is the Landé factor and μ_K the effective moment of the Kondo ion. The result of fit of H^* to Eq. (15) yields values of $T_K = -14$ K and the effective moment of the Kondo ion $\mu_K = 0.2\ \mu_B$. A negative value of T_K was previously observed

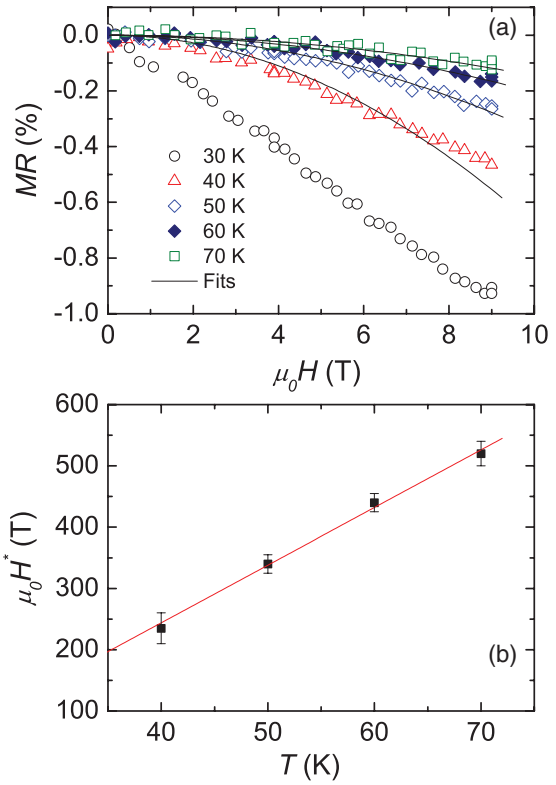

FIG. 11. (Color online) (a) The MR isotherms of U_2Pt_2Sn at various temperatures. The solid lines are fits to Eq. (14). (b) Characteristic field H^* obtained from the fits as a function of temperature.

in uranium-based Kondo-lattice compound UBe_{13},[67] in which the behavior was interpreted as due to ferromagnetic correlations. Thus, the negative value of T_K in U_2Pt_2Sn is consistent with the specific-heat data. The presence of a ferromagnetic interaction is presumably due to the canted antiferromagnetic structure, which was previously reported.[13] To analyze the magnetoresistance data in terms of the Schlottmann model, we have made two assumptions. The first was that the field dependence of the resistivity of U_2Pt_2Sn above 40 K originates from the single-ion Kondo scattering, and other mechanisms are negligible. The second assumption was an effective $J = 1/2$ moment for the ground state. Justification for the latter may be based on the specific-heat results presented above.

E. Discussion

From the present results, we can propose that the antiferromagnetic U_2Pt_2Sn with $T_N = 15.7$ K is a dense Kondo compound, in which the Kondo effect with the Kondo temperature $T_K \sim 30$ K competes with exchange interactions. In the framework of the classical Kondo-lattice model of Doniach,[1] one qualitatively explains the experimental observations, such as low-temperature magnetic ordering, reduced magnetic moment, enhanced electronic contribution to the specific heat, and reduced entropy at the ordering temperature. In such an approach, the Kondo effect is basically responsible for the heavy-fermion properties. However, in order to discriminate heavy-fermion between other scenarios leading to the enhancement in the Sommerfeld ratio, let us combine the specific-heat results with the susceptibility and with the electrical resistivity. Within the Landau Fermi-liquid theory, the electronic correlations renormalize the quasiparticle effective mass, and then enhance both the zero-temperature susceptibility $\chi(0)$, the Sommerfeld ratio γ, and the quadratic term of the resistivity A. It is known that the Wilson ratio

$$R_W = \left(\frac{\pi k_B}{\mu_{\rm eff}}\right)^2 \frac{\chi(0)}{3\gamma} \tag{16}$$

for a noninteracting Fermi gas equal to 1. Furthermore, in a system where electron-phonon interactions enhance γ but not $\chi(0)$, there will be a reduction of R_W. Conversely, when spin-spin interactions are strong, R_W becomes enhanced. For Kondo systems, the Wilson ratio of 2 is expected.[20] Taking $\gamma = 150$ mJ/mol$_U$ K^2 and the value $\chi_{\rm poly}$ at 2 K $= 11.2$ cm^3/mol$_U$ and $\mu_{\rm eff} = 2.4\ \mu_B$, we estimated $R_W = 2.8$ for U_2Pt_2Sn, being comparable to those observed in many heavy fermions.[68] An enhancement in R_W of U_2Pt_2Sn may indicate the importance of ferromagnetic correlations taking place in U_2Pt_2Sn at low temperatures.

A heavy-fermion state in strongly correlated electron metals can be characterized by the Kadowaki-Woods (KW) ratio $A/\gamma^2 = 1 \times 10^{-5}\ \mu\Omega$ cm/(mJ/mol K)^2.[69] A is the coefficient of the T^2 dependence of the resistivity and thus denotes electron-electron interactions. The electronic specific-heat coefficient γ is simply a direct measure of the effective mass m^* of quasiparticles, which is about 75 m_e in U_2Pt_2Sn. It has been shown by Tsujii *et al.*[70] that the A/γ^2 ratio depends on the carrier density n and the ground-state degeneracy $N = 2J + 1$ as

$$\frac{A}{\gamma^2} = \frac{h}{e^2 K_B^2 N_A^2} \frac{9(3\pi)^{-1/3}}{n^{4/3} a^3} \frac{1}{\frac{1}{2}N(N-1)}. \tag{17}$$

For $n = 2$ and $n^{4/3}a^3 = 1 \times 10^8$ cm^{-1}, the formula meets the KW ratio. According to the authors, the n dependence of A/γ^2 is qualitatively consistent with the Kondo resonance picture. When $n = 2$, the Kondo resonance peak is situated at the Fermi energy level E_F. For large $N = 4,6,8$, the resonance peak develops at an energy larger than E_F. So, the resulting band shape can reduce the value A/γ^2. In U_2Pt_2Sn, this ratio can be estimated from $a = 0.48\ \mu\Omega$ cm/K^2 and $\gamma = 150$ mJ/mol$_U$ K^2 to be $2.15 \times 10^{-5}\ \mu\Omega$ cm/(mJ/mol K)^2. The result classifies U_2Pt_2Sn to belong to a class of strong-coupling compounds with the degeneracy $N = 2$, i.e., doublet CEF configuration. It is worthwhile to add that the magnifying of the A/γ^2 value in U_2Pt_2Sn, according to Eq. (17), is related to a small carrier density of the compound.

One of the remarkable findings in this work is the scaling behavior of the Kondo-liquid contribution of the Knight shift of U_2Pt_2Sn with a characteristic temperature $T^* = 80$ K. This result indicates that likewise the Kondo temperature T_K, T^* is a condensation energy scale, and suggesting to check the relationship between T^* and T_K. Taking the T_K values for uranium-based heavy-fermion compounds from literature, such as URu_2Si_2 ($T_K \sim 60$ K),[71] UBe_{13} ($T_K \sim 5.5$ K),[72] and UPt_3 ($T_K \sim 10$ K),[73] and the corresponding T^* values from work of Curro *et al.*[54] we plot T^* versus T_K in Fig. 12. In this figure, we plot also the dashed line for the ratio $R = T^*/T_K = 2$ as a guide to the eye. Apparently, the available literature data together with that of U_2Pt_2Sn lie approximately on the same

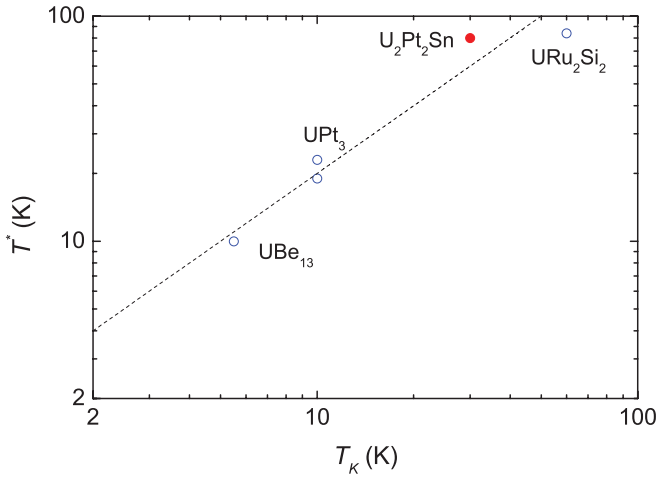

FIG. 12. (Color online) T^* vs T_K of U_2Pt_2Sn is compared with those of uranium-based heavy-fermion compounds. The dashed line shows $T^*/T_K = 2$.

line. This could be a next support that the studied U_2Pt_2Sn compound belongs to the class of heavy-fermion U-based materials. It is hoped that further comparative studies of the ratio $R = T^*/T_K$ should give a more detailed information about the relationship between the magnitudes of R and the occurrence of intermediate valence, heavy-fermion, and quantum criticality phenomena.

In conclusion, we have presented the measurements of magnetization, specific heat, ^{195}Pt and ^{119}Sn NMR Knight shift, resistivity, and magnetoresistance for U_2Pt_2Sn. The main result obtained from this work is to have shown that the physical properties of U_2Pt_2Sn are governed by an interplay between long-range AF interaction, Kondo and CEF effects. We have found that it is essential to use the spin-wave theory in order to obtain a consistent description of the zero-field specific heat and electrical resistivity in the antiferromagnetic state. Our experimental data point out that the Kondo effect with $T_K \sim 30$ K is responsible for the development of the heavy-fermion state in this compound. This work highlights the fact that the Kondo-lattice component of the ^{195}Pt and ^{119}Sn NMR Knight shift follows the expression $K_{\mathrm{KL}} \propto (1 - T/T^*)\ln(T^*/T)$ derived from the two-fluid model for heavy fermions. For U_2Pt_2Sn, it is found $T^* \sim 80$ K, indicative of strongly electron correlations below this temperature. We propose thus to test the ratio T^*/T_K for other strongly correlated materials in order to establish an eventual relationship between R values and the occurrence of various exotic phenomena in strongly correlated electron materials.

ACKNOWLEDGMENT

We would like to thank L. Kępiński and E. Bukowska for performing SEM/EDX and x-ray powder diffraction measurements, respectively.

[1] S. Doniach, in *Valence Instabilities and Related Narrow Band Phenomena*, edited by R. D. Parks (Plenum, New York, 1977), p. 169; Phys. B (Amsterdam) **91**, 231 (1977).
[2] H. Nakotte, K. Prokeš, E. Brück, N. Tang, F. R. de Boer, P. Svoboda, V. Sechovský, L. Havela, J. M. Winand, A. Seref, J. Rebizant, and J. C. Spirlet, Phys. B (Amsterdam) **201**, 247 (1994).
[3] L. Havela, V. Sechovský, P. Svoboda, H. Nakotte, K. Prokeš, F. R. de Boer, A. Seret, J. M. Winand, J. Rebizant, J. C. Spirlet, A. Purwanto, and R. A. Robinson, J. Magn. Magn. Mater. **140-144**, 1367 (1995).
[4] P. Estrela, Ph.D. thesis, University of Amsterdam, 2000 [http://opus.bath.ac.uk/15350/1/estrela-thesis.pdf].
[5] V. H. Tran, Z. Żołnierek, A. J. Zaleski, and H. Noël, Solid State Commun. **101**, 709 (1997).
[6] P. deV. du Plessis, A. M. Strydom, and V. H. Tran, Solid State Commun. **112**, 391 (1999).
[7] V. H. Tran and E. Bauer, J. Phys.: Condens. Matter **18**, 4677 (2006).
[8] P. Estrela, A. de Visser, F. R. de Boer, G. J. Nieuwenhuys, L. C. J. Pereira, and M. Almeida, Phys B: Condens. Matter **259-261**, 409 (1999).
[9] A. M. Strydom and P. de V. du Plessis, Phys. B: Condens. Matter **230-232**, 62 (1997).
[10] L. C. J. Pereira, J. M. Winand, F. Wastin, J. Rebizant, and J. C. Spirlet, in Proceedings of the 24th Journèes des Actinides, Obergurgl, Austria, 1994 (unpublished).
[11] P. Gravereau, F. Mirambet, B. Chevalier, F. Weill, L. Fournès, D. Laffargue, F. Bourée, and J. Etourneau, J. Mater. Chem. **4**, 1893 (1994).
[12] Z. Żołnierek and A. Zaleski, in Proceedings of the 23rd Journées des Actinides, Schwarzwald, Germany, 1993 (unpublished).
[13] K. Prokeš, P. Svoboda, A. Kolomiets, V. Sechovský, H. Nakotte, F. R. de Boer, J. M. Winand, J. Rebizant, and J. C. Spirlet, J. Magn. Magn. Mater. **202**, 451 (1999).
[14] K. Prokeš, F. R. de Boer, H. Nakotte, L. Havela, V. Sechovský, P. Svoboda, J. M. Winand, J. Rebizant, J. C. Spirlet, X. Hu, and T. J. Gortenmulder, J. Appl. Phys. **79**, 6361 (1996).
[15] A. M. Strydom and P. de V. du Plessis, Solid State Commun. **102**, 307 (1997).
[16] T. Roisnel and J. Rodriguez-Carvajal, Mater. Sci. Forum **378-381**, 118 (2001).
[17] R. K. Harris, E. D. Becker, S. M. Cabral de Menezes, R. Goodfellow, and P. Granger, Solid State Nucl. Magn. Reson. **22**, 458 (2002); Pure Appl. Chem. **73**, 1795 (2001).
[18] R. K. Harris, E. D. Becker, S. Cabral de Menezes, R. Goodfellow, P. Granger, and R. E. Hoffman, Solid State Nucl. Magn. Reson. **33**, 41 (2008); Pure Appl. Chem. **80**, 59 (2008).
[19] B. Nowak, Solid State Nucl. Magn. Reson. **37**, 36 (2010).
[20] A. C. Hewson, *The Kondo Problem to Heavy Fermions* (Cambridge University Press, Cambridge, England, 1993).
[21] J. C. Gómez Sal, J. García Soldevilla, J. A. Blanco, J. I. Espeso, J. Rodríguez Fernández, F. Luis, F. Bartolomé, and J. Bartolomé, Phys. Rev. B **56**, 11741 (1997).
[22] P. Sun, Y. Isikawa, Q. Lu, D. Huo, and T. Kuwai, J. Phys. Soc. Jpn. **72**, 916 (2003).
[23] M. E. Fisher, Philos. Mag. **7**, 1731 (1962).

[24]V. H. Tran, S. Paschen, A. Rabis, N. Senthilkumaran, M. Baenitz, F. Steglich, P. de V. du Plessis, and A. M. Strydom, Phys. Rev. B **67**, 075111 (2003).
[25]M. Bouvier, P. Lethuillier, and D. Schmitt, Phys. Rev. B **43**, 13137 (1991).
[26]A. Purwanto, R. A. Robinson, L. Havela, V. Sechovsky, P. Svoboda, H. Nakotte, K. Prokes, F. R. de Boer, A. Seret, J. M. Winand, J. Rebizant, and J. C. Spirlet, Phys. Rev. B **50**, 6792 (1994).
[27]E. S. R. Gopal, *Specific Heats at Low Temperatures* (Heykood Books, London, 1966).
[28]C. D. Bredl, F. Steglich, and K. D. Schotte, Z. Phys. B: Condens. Matter Quanta **29**, 327 (1978).
[29]J. A. Blanco, M. de Podesta, J. I. Espeso, J. C. Gómez Sal, C. Lester, K. A. McEwen, N. Patrikios, and J. Rodríguez Fernández, Phys. Rev. B **49**, 15 126 (1994).
[30]H. Yashima, H. Mori, N. Sato, and T. Satoh, J. Magn. Magn. Mater. **31–34**, 411 (1983).
[31]V. T. Rajan, Phys. Rev. Lett. **51**, 308 (1983).
[32]A. I. Akhiezer, V. G. Bar′yakhtar, and M. I. Kaganov, Usp. Fiz. Nauk **71**, 533 (1960) [Sov. Phys. Usp. **3**, 567 (1961)].
[33]L. J. Sundströ, in *Handbook on the Physics and Chemistry of Rare Earths*, edited by K. A. Gschneidner Jr. and L. Eyring (Elsevier, Amsterdam, 1979), Vol. 1, Chap.5, p. 379.
[34]J. G. Serenic, *Encyclopedia of Materials: Sciences and Technology* (Elsevier, Amsterdam, 2001), p. 4986.
[35]R. Felten, F. Steglich, G. Weber, H. Riefschel, F. Goupf, B. Renker, and J. Beuers, Europhys. Lett. **2**, 323 (1986).
[36]H. E. Fischer, E. T. Swartz, R. O. Pohl, B. A. Jones, J. W. Wilkins, and Z. Fisk, Phys. Rev. B **36**, 5330 (1987).
[37]R. Burriel, M. To, H. Zainel, E. F. Westrum Jr., E. H. P. Cordfunke, R. P. Muis, and G. Wijbenga, J. Chem. Thermodynam. **20**, 815 (1988).
[38]G. C. Carter, L. H. Bennett, and D. J. Kahan, Prog. Mater. Sci. **20**, 1 (1977).
[39]Y. Kohori, M. Kyogaku, T. Kohara, K. Asayama, H. Amitsuka, and Y. Miyako, J. Magn. Magn. Mater. **90-91**, 510 (1990).
[40]M. Lee, G. F. Moores, Y.-Q. Song, W. P. Halperin, W. W. Kim, and G. R. Stewart, Phys. Rev. B **48**, 7392 (1993).
[41]A. Grykałowska and B. Nowak, J. Alloys Compd. **453**, 7 (2008).
[42]K. Kojima, T. Takabatake, A. Harada, and T. Hihara, Phys B (Amsterdam) **206-207**, 479 (1995).
[43]B. Nowak, Phys. Rev. B **83**, 134102 (2011).
[44]M. Benakki, A. Qachaou, and P. Panissod, J. Magn. Magn. Mater. **73**, 141 (1988).
[45]K. Kojima, Y. Hukuda, S. Miyata, T. Takabatake, H. Fujii, and T. Hihara, J. Magn. Magn. Mater. **104-107**, 49 (1992).
[46]K. Kojima, Y. Hukuda, S. Miyata, T. Takabatake, H. Fujii, and T. Hihara, J. Phys. Soc. Jpn. **60**, 2546 (1991).
[47]M. J. Lysak and D. E. MacLaughlin, Phys. Rev. B **31**, 6963 (1985).
[48]D. E. MacLaughlin, Hyperfine Interact. **49**, 43 (1989).
[49]D. E. MacLaughlin, J. Magn. Magn. Mater. **47-48**, 121 (1985).
[50]T. Ohama, H. Yasuoka, D. Mandrus, Z. Fisk, and J. L. Smith, J. Phys. Soc. Jpn. **64**, 2628 (1995).
[51]A. Schenck, N. K. Sato, G. Solt, D. Andreica, F. N. Gygax, M. Pinkpank, and A. Amato, Eur. Phys. J. B **13**, 245 (2000).
[52]E. Kim, M. Makivic, and D. L. Cox, Phys. Rev. Lett. **75**, 2015 (1995).
[53]S. Nakatsuji, D. Pines, and Z. Fisk, Phys. Rev. Lett. **92**, 016401 (2004).
[54]N. J. Curro, B.-L. Young, J. Schmalian, and D. Pines, Phys. Rev. B **70**, 235117 (2004).
[55]N. J. Curro, B.-L. Young, J. Schmalian, and D. Pines, Phys. B (Amsterdam) **378-380**, 754 (2006).
[56]Y.-F. Yang and D. Pines, Phys. Rev. Lett. **100**, 096404 (2008).
[57]N. apRoberts-Warren, A. P. Dioguardi, A. C. Shockley, C. H. Lin, J. Crocker, P. Klavins, D. Pines, N. J. Curro, and Y.-F. Yang, Phys. Rev. B **83**, 060408(R) (2011).
[58]E. Fawcett, H. L. Alberts, V. Yu. Galkin, D. R. Noakes, J. V. Yakhmi, Rev. Mod. Phys. **66**, 25 (1994).
[59]M. A. Continentino, S. N. de Medeiros, M. T. D. Orlando, M. B. Fontes, and E. M. Baggio-Saitovitch, Phys. Rev. B **64**, 012404 (2001).
[60]E. Jobiliong, J. S. Brooks, E. S. Choi, H. Lee, and Z. Fisk, Phys. Rev. B **72**, 104428 (2005).
[61]N. H. Andersen, in *Crystalline Field and Structural Effects in f-Electron Systems*, edited by J. E. Crow, R. P. Guertin, and T. W. Mihalism (Plenum, New York, 1980), p. 373.
[62]T. T. M. Palstra, A. A. Menovsky, and J. A. Mydosh, Phys. Rev. B **33**, 6527 (1986).
[63]T. Kawai, Y. Okuda, H. Shishido, A. Thamizhavel, T. D. Matsuda, Y. Haga, M. Nakashima, T. Takeuchi, M. Hedo, Y. Uwatoko, R. Settai, and Y. Onuki, J. Phys. Soc. Jpn. **76**, 014710 (2007).
[64]P. Schlottmann, Z. Phys. B: Condens. Matter **51**, 223 (1983).
[65]N. Andrei, K. Furuya, and J. H. Lowenstein, Rev. Mod. Phys. **55**, 331 (1983).
[66]B. Batlogg, D. J. Bishop, E. Bucher, B. Golding Jr., A. P. Ramirez, Z. Fisk, J. L. Smith, and H. R. Ott, J. Magn. Magn. Mater. **63–64**, 441 (1987).
[67]B. Andraka and G. R. Stewart, Phys. Rev. B **49**, 12359 (1994).
[68]Z. Fisk, H. R. Ott, and G. Aeppli, Jpn. J. Appl. Phys. Suppl. **26**, 1882 (1987).
[69]K. Kadowaki and S. B. Woods, Solid State Commun. **58**, 507 (1986).
[70]N. Tsujii, H. Kontani, and K. Yoshimura, Phys. Rev. Lett. **94**, 057201 (2005).
[71]T. Kohara, Y. Kohori, K. Asayama, Y. Kitaoka, M. B. Maple, and M. S. Torikachvili, Solid State Commun. **59**, 603 (1986).
[72]M. C. Aronson, J. D. Thompson, J. L. Smith, Z. Fisk, and M. W. McElfresh, Phys. Rev. Lett. **63**, 2311 (1989).
[73]A. J. Arko, J. J. Joyce, A. B. Andrews, J. D. Thompson, J. L. Smith, D. Mandrus, M. F. Hundley, A. L. Cornelius, E. Moshopoulou, Z. Fisk, P. C. Canfield, and A. Menovsky, Phys. Rev. B **56**, R7041 (1997).